

# Quality Factor of Nanobowtie Antenna

Chi-Yu Adrian Ni, Shu-Wei Chang, *Member, IEEE*, Shun Lien Chuang *Fellow, IEEE*, and P. James Schuck

**Abstract**—We present a rigorous formulation based on the Poynting’s theorem in dispersive and lossy media to calculate the quality factor, material loss, radiation loss, and radiation pattern of an optical nanobowtie antenna using the finite-difference time-domain method. The quality factor obtained from our theory, 8.73, agrees well with the experimental data. Our results show that the radiation loss and material loss are comparable. The material loss mainly originates from the chromium rather than gold even though the nanobowtie antenna mostly consists of gold. In addition, due to the small gap and plasmonic mode confinement, the effective modal volume is ultrasmall [ $6.36 \times 10^{-5} (\lambda/n_{\text{eff}})^3$ ], which significantly breaks the diffraction limit.

**Index Terms**—Bowtie antenna, finite-difference-time-domain method, quality factor.

## I. INTRODUCTION

NANO-bowtie antennas are widely investigated because of their high local field enhancement and nanoscale light confinement due to the surface plasmons. Their characteristics such as the dependence of the resonance wavelength on the gap distance have been experimentally and theoretically demonstrated [1], [2]. Recently, the effect of dielectric coating on metallic bowtie nanoantennas is also investigated and the theory shows an excellent agreement with the experiment [3]. Near the tip, the bowtie antenna with a gap size smaller than 20 nm can reach an intensity enhancement of more than 1000 [1]. The improvement of intensity enhancement over 16 times by using the triangle aperture compared with the rectangular aperture on the surface of the vertical cavity surface emitting laser (VCSEL) was also reported [4]. Owing to the high intensity enhancement, the nanobowtie antenna can be designed to enhance the signal from molecules [5], [6]. A recent experiment has also shown that cross nanobowtie antennas can not only capture and confine the optical field in nanoscale, but also filter and manipulate it spectrally [7]. Experimentally, nanobowtie antennas can shrink the field size down to about one fiftieth to one thirtieth of the wavelengths in mid-infrared regime [8]. So far, most attention on the nanobowtie antenna is focused on its large intensity enhancement and capability of shrinking the field size. Its quality factor ( $Q$ ), however, is less studied. Recently, the bowtie nanolaser has been proposed [9] since the nanobowtie antenna is expected to provide an ultrasmall effective modal volume ( $V_{\text{eff}}$ ). A device with a large  $Q/V_{\text{eff}}$  ratio could possibly make a nanolaser. Compared to the quality factors of conventional lasers, the nanobowtie

antenna has a much smaller  $Q$  of around 10. Even with such a small  $Q$ , the large field enhancement of the bowtie antenna can reduce the effective modal volume down to the sub-wavelength regime and sustain a decent  $Q/V_{\text{eff}}$  ratio. The ultrasmall optical modal volume and thresholdless behavior have been examined based on the rigorous rate equations with the dispersive media taken into account [9], [10], in which the knowledge of the quality factor is important for the evaluation of device performances.

An appropriate definition of the electric energy density is very important in the calculation of  $Q$  and field normalization, especially in the dispersive media. Many works have addressed the definition of the electric energy in dispersive media [11]–[16]. When the frequency of interest is much larger than the material damping (dissipation) and far away from the transition frequencies corresponding to bands of materials, the common definition of electric energy in a dispersive medium gives a positive energy [11], [12]:

$$\langle U_e \rangle \simeq \int_V d\mathbf{r} \frac{\epsilon_0}{2} \frac{\partial[\omega \epsilon_{r,R}(\mathbf{r}, \Omega)]}{\partial \omega} \Big|_{\omega=\omega_0} \langle \mathbf{E} \cdot \mathbf{E} \rangle \quad (1)$$

where  $\epsilon_{r,R}$ ,  $\omega_0$  is the real part of the relative permittivity (denoted by the subscript  $r$ ) and the carrier frequency of the field, respectively; and  $\langle \dots \rangle$  means the time average over half an optical period  $T = \pi/\omega_0$ . The slope of  $\epsilon_{r,R}$  with respect to the angular frequency  $\omega$  is often positive, and thus a positive time-averaged electric energy. However, when the frequency of interest is around the transition frequencies, the slope may be negative and lead to a nonphysical negative energy. In that case, a more appropriate definition has to be used.

In this paper, we adopt a rigorous formulation to calculate the electric energy based on the *Poynting’s theorem in dispersive and lossy media* and apply it to a nanobowtie antenna consisting of a thin adhesive layer of chromium and a thick layer of gold. The frequency of interest in this work is far away from the transition frequency of gold, and the expression of electric energy in (1) can be applied. However, this frequency is around the transition frequency of chromium, which requires the Drude term and at least one Lorentz term for narrowband modeling. Therefore, a proper definition of effective energy which incorporates these two types of terms [13]–[16] is necessary in our calculation. For generality, we will use an improved definition of electric energy than (1) for both gold and chromium. Based on the finite-difference time-domain (FDTD) method [17], we apply this formulation to analyze the quality factor of the nanobowtie antenna and other quantities such as radiation loss, absorption loss, and radiation pattern using a software package with subpixel smoothing for increased accuracy [18]. The FDTD method also allows us to obtain the intrinsic performance for this open cavity by turning off the sinusoidal excitation source and obtain the true mode pattern

This work at the University of Illinois at Urbana-Champaign and Lawrence Berkeley National Laboratory was supported by the DARPA NACHOS Program.

C. Y. A. Ni, S. W. Chang, and S. L. Chuang are with the Department of Electrical and Computer Engineering, University of Illinois at Urbana-Champaign, Urbana, IL 61801, USA (e-mail: s-chuang@illinois.edu). P. J. Schuck and others are with Lawrence Berkeley National Laboratory, Berkeley, CA 94720, USA.

without the interference of the incident source field. Without the interference of the source, the calculated energy is more reliable, and so are the calculations of confinement factors and effective modal volumes. The effective modal volume is very small and significantly breaks the diffraction limit, i.e., half wavelengths in all three dimensions. This investigation is beneficial to the design and characterization of optical nanoantennas.

## II. THEORY

The quality factor of a cavity mode in the frequency domain is defined as

$$Q = \frac{\omega_0 U}{P} \quad (2)$$

where  $\omega_0$  is the resonance angular frequency of the mode,  $U$  is the corresponding stored energy, which accounts for the dispersive material, and  $P$  is the time-averaged power loss including the radiation loss  $P_{\text{rad}}$  and absorption loss  $P_{\text{abs}}$  from the cavity:

$$P = P_{\text{rad}} + P_{\text{abs}} \quad (3)$$

The quality factor  $Q$  can also be decomposed into two contributions:

$$\frac{1}{Q} = \frac{1}{Q_{\text{rad}}} + \frac{1}{Q_{\text{abs}}} \quad (4)$$

where  $Q_{\text{rad}}$  and  $Q_{\text{abs}}$  are due to the radiation and absorption losses, respectively, and are defined as

$$Q_{\text{rad}} = \frac{\omega_0 U}{P_{\text{rad}}} \quad (5)$$

$$Q_{\text{abs}} = \frac{\omega_0 U}{P_{\text{abs}}} \quad (6)$$

Once we can obtain the exact field distributions of the cavity mode, such as the mode in a perfect electric conductor (PEC) cavity, the stored energy as well as radiation and absorption losses can be obtained [19]. The quality factor can then be calculated according to (5) and (6). This method is effective only when the electric and magnetic fields of the cavity modes are known. For the complicated quasi-bounded modes of a nanobowtie antenna, various physical quantities are difficult to obtain in the three-dimensional space. Therefore, this approach is not easily applicable, though not impossible.

Another approach is to calculate the quality factor in the time domain. A few algorithms have been used based on FDTD [20]–[22] and the Poynting's theorem to calculate the quality factor with their validity successfully demonstrated. However, in those cases, metals are considered as PEC, and therefore they cannot be directly applied to nanobowtie antennas since at optical wavelengths, the material dispersion of metal comes into play. Another method is to send a short pulse into the cavity, and the signal in the time domain is then converted to its counterpart in the frequency domain via the Fourier transform. Based on the frequency components of the signal, the resonance frequencies and the quality factors corresponding to different modes are extracted by finding the complex frequencies, for example, with the filter-diagonalization method [23]. This method is efficient when the quality factor is large but becomes inaccurate for a lossy

cavity due to the difficulty in distinguishing the weak signal from noise.

On the other hand, the quality factor can be directly calculated using the Poynting's theorem. The advantage of using Poynting's theorem is that it not only gives the quality factor but also provides explicitly the absorption and radiation losses. In our wavelengths of interest, the plasmonic effect is present, and the dispersion of the metal has to be taken into account. In this work, we use a definition of the electric energy consistent with the Poynting's theorem including the Drude and Lorentz models. This definition gives a close result to that of (1) if the frequency of interest is much larger than the material damping and far away from the transition frequencies of metals.

The Poynting's theorem in dispersive and inhomogeneous media [11], [12] is:

$$\frac{\partial}{\partial t} \langle U_{\text{total}} \rangle = \frac{\partial}{\partial t} (\langle U_e \rangle + \langle U_m \rangle) \simeq -\langle P_{\text{rad}} \rangle - \langle P_{\text{abs}} \rangle \quad (7a)$$

$$\begin{aligned} \langle U_e \rangle &= \int_V d\mathbf{r} \frac{\epsilon_0}{4} \frac{\partial[\omega \epsilon_{r,R}(\mathbf{r}, \omega)]}{\partial \omega} \Big|_{\omega=\omega_0} |\mathbf{E}_s|^2 \\ &\simeq \int_V d\mathbf{r} \frac{\epsilon_0}{2} \frac{\partial[\omega \epsilon_{r,R}(\mathbf{r}, \omega)]}{\partial \omega} \Big|_{\omega=\omega_0} \langle \mathbf{E} \cdot \mathbf{E} \rangle \end{aligned} \quad (7b)$$

$$\langle U_m \rangle = \int_V d\mathbf{r} \frac{\mu_0}{4} |\mathbf{H}_s|^2 \simeq \int_V d\mathbf{r} \frac{\mu_0}{2} \langle \mathbf{H} \cdot \mathbf{H} \rangle \quad (7c)$$

$$\langle P_{\text{rad}} \rangle = \left\langle \oint_S d\mathbf{s} \cdot (\mathbf{E} \times \mathbf{H}) \right\rangle \quad (7d)$$

$$\begin{aligned} \langle P_{\text{abs}} \rangle &= \int_V d\mathbf{r} \frac{\omega_0 \epsilon_0 \epsilon_{r,I}(\mathbf{r}, \omega_0)}{2} |\mathbf{E}_s|^2 \\ &\simeq \int_V d\mathbf{r} \omega_0 \epsilon_0 \epsilon_{r,I}(\mathbf{r}, \omega_0) \langle \mathbf{E} \cdot \mathbf{E} \rangle \end{aligned} \quad (7e)$$

where  $\omega_0$  is the resonance angular frequency;  $S$  is the surface enclosing  $V$ ;  $\epsilon_{r,R}(\mathbf{r}, \omega)$  is the real part of the relative permittivity function;  $\epsilon_{r,I}(\mathbf{r}, \omega)$  is the imaginary counterpart;  $\partial[\omega \epsilon_{r,R}(\mathbf{r}, \omega)]/\partial \omega$  is the group permittivity [10];  $\langle U_e \rangle$ ,  $\langle U_m \rangle$ , and  $\langle U_{\text{total}} \rangle$  are the time-averaged electric, magnetic, and total energies, respectively;  $\langle P_{\text{rad}} \rangle$  and  $\langle P_{\text{abs}} \rangle$  represent the time-averaged radiation and absorption powers; and a physical quantity  $\mathbf{A}(\mathbf{r}, t)$  with slowly-varying part  $\mathbf{A}_s(\mathbf{r}, t)$  is defined as

$$\mathbf{A}(\mathbf{r}, t) = \frac{1}{2} [\mathbf{A}_s(\mathbf{r}, t) e^{-i\omega_0 t} + \mathbf{A}_s^*(\mathbf{r}, t) e^{i\omega_0 t}] \quad (8)$$

Although (7a)–(7e) can be used in most optic applications, the group permittivity in (7b) is not always positive. Therefore, an alternative definition [13]–[16], which is dedicated to the Drude or Lorentz model and does not have the issue such as negative energy, has to be used. To obtain the more general definition, we start from the instantaneous Poynting's theorem:

$$-\int_V d\mathbf{r} \left[ \mathbf{E} \cdot \frac{\partial \mathbf{D}}{\partial t} + \mathbf{H} \cdot \frac{\partial \mathbf{B}}{\partial t} \right] = \int_V d\mathbf{r} \nabla \cdot (\mathbf{E} \times \mathbf{H}) \quad (9)$$

The first term inside the bracket of the left-hand side in (9) can be rewritten as:

$$\mathbf{E} \cdot \frac{\partial \mathbf{D}}{\partial t} = \mathbf{E} \cdot \frac{\partial}{\partial t} [\epsilon_\infty \mathbf{E} + \mathbf{P}] = \epsilon_\infty \mathbf{E} \cdot \frac{\partial \mathbf{E}}{\partial t} + \mathbf{E} \cdot \frac{\partial \mathbf{P}}{\partial t} \quad (10)$$

where  $\mathbf{P}$  is the polarization and  $\epsilon_\infty = \epsilon_0 \epsilon_{r,\infty}$  is the background permittivity and  $\epsilon_{r,\infty}$  is the *relative* background permittivity and includes the contributions from other polarizations. For an explicit expression of the last term in (10),

we consider both the Lorentz and Drude models. The two models are widely used to describe the dispersive property of metals [24]. For simplicity, we first consider Lorentz and Drude models separately and obtain a more general expression later.

In the Lorentz model, each electron is considered as a non-interacting but damped oscillator, which is driven by the electric field [13]. The equation of motion for an electron is:

$$m \left( \frac{\partial^2 \mathbf{x}}{\partial t^2} + \gamma_1 \frac{\partial \mathbf{x}}{\partial t} + \omega_1^2 \mathbf{x} \right) = -f_1 q \mathbf{E} \quad (11)$$

where  $\mathbf{x}$ ,  $m$ ,  $\gamma_1$ ,  $\omega_1$ , and  $f_1$  are the displacement, the mass of a single electron, damping factor, transition frequency, and the oscillation strength, respectively [24]. The relation of the polarization  $\mathbf{P}_L$  in the Lorentz model with the displacement  $\mathbf{x}$  is:

$$\mathbf{P}_L = -Nq\mathbf{x} \quad (12)$$

where  $N$  is the total number of electrons. Therefore, we can rewrite (11) in terms of  $\mathbf{P}_L$  as

$$\frac{\partial^2 \mathbf{P}_L}{\partial t^2} + \gamma_1 \frac{\partial \mathbf{P}_L}{\partial t} + \omega_1^2 \mathbf{P}_L = f_1 \epsilon_0 \omega_p^2 \mathbf{E} \quad (13)$$

where  $\omega_p = \sqrt{Nq^2/m\epsilon_0}$  is the plasma frequency. After an inner product of the time derivative  $\partial \mathbf{P}_L / \partial t$  on both sides of (13), we obtain the following equation:

$$\frac{\partial}{\partial t} \left[ \frac{1}{2} \left| \frac{\partial \mathbf{P}_L}{\partial t} \right|^2 + \frac{1}{2} \omega_1^2 |\mathbf{P}_L|^2 \right] + \gamma_1 \left| \frac{\partial \mathbf{P}_L}{\partial t} \right|^2 = f_1 \epsilon_0 \omega_p^2 \mathbf{E} \cdot \frac{\partial \mathbf{P}_L}{\partial t} \quad (14)$$

For the Drude model, we obtain a similar equation by setting the transition frequency to zero:

$$\frac{\partial}{\partial t} \left[ \frac{1}{2} \left| \frac{\partial \mathbf{P}_D}{\partial t} \right|^2 \right] + \gamma_0 \left| \frac{\partial \mathbf{P}_D}{\partial t} \right|^2 = f_0 \epsilon_0 \omega_p^2 \mathbf{E} \cdot \frac{\partial \mathbf{P}_D}{\partial t} \quad (15)$$

where the subscript ‘‘D’’ denotes the Drude model; and  $\gamma_0$  and  $f_0$  are the damping factor and oscillator strength corresponding to the Drude model.

If only the Drude damping and one Lorentz type of transition are included, the total polarization is the sum of  $\mathbf{P}_L$  and  $\mathbf{P}_D$ . Therefore, (10) is written as

$$\begin{aligned} \mathbf{E} \cdot \frac{\partial [\epsilon_\infty \mathbf{E} + \mathbf{P}]}{\partial t} &= \frac{\partial}{\partial t} \left( \frac{1}{2} \epsilon_\infty |\mathbf{E}|^2 \right) + \mathbf{E} \cdot \frac{\partial (\mathbf{P}_L + \mathbf{P}_D)}{\partial t} \\ &= \frac{\partial}{\partial t} \left\{ \frac{1}{2} \epsilon_\infty |\mathbf{E}|^2 + \frac{1}{f_0 \epsilon_0 \omega_p^2} \frac{1}{2} \left| \frac{\partial \mathbf{P}_D}{\partial t} \right|^2 \right. \\ &\quad \left. + \frac{1}{f_1 \epsilon_0 \omega_p^2} \frac{1}{2} \left[ \left| \frac{\partial \mathbf{P}_L}{\partial t} \right|^2 + \omega_1^2 \mathbf{P}_L^2 \right] \right\} \\ &\quad + \frac{\gamma_0}{f_0 \epsilon_0 \omega_p^2} \left| \frac{\partial \mathbf{P}_D}{\partial t} \right|^2 + \frac{\gamma_1}{f_1 \epsilon_0 \omega_p^2} \left| \frac{\partial \mathbf{P}_L}{\partial t} \right|^2 \end{aligned} \quad (16)$$

We can set the terms in the curly brackets of (16) as the electric energy density and the last two terms as the absorption loss. If we consider the sinusoidal steady state with a time dependence  $\exp(-i\omega t)$ , (11) can be converted to the phasor form:

$$m [-\omega^2 \mathcal{X} - i\omega\gamma_1 \mathcal{X} + \omega_1^2 \mathcal{X}] = -f_1 q \mathcal{E} \quad (17)$$

where  $\mathcal{X}$  and  $\mathcal{E}$  are the phasors of  $\mathbf{x}$  and  $\mathbf{E}$ , respectively. With some algebra, we rewrite the phasor  $\mathcal{X}$  as

$$\mathcal{X} = \frac{-f_1 q / m}{\omega_1^2 - \omega^2 - i\omega\gamma_1} \mathcal{E} \quad (18)$$

From (18) and (12), the polarization phasor  $\mathcal{P}_L$  for the Lorentz model becomes

$$\mathcal{P}_L = -Nq\mathcal{X} = \frac{f_1 \epsilon_0 \omega_p^2}{\omega_1^2 - \omega^2 - i\omega\gamma_1} \mathcal{E} \quad (19)$$

The phasor of the derivative of  $\mathbf{P}_L$  with respect to time can then be represented as

$$-i\omega \mathcal{P}_L = i\omega Nq\mathcal{X} = \frac{-i\omega f_1 \epsilon_0 \omega_p^2}{\omega_1^2 - \omega^2 - i\omega\gamma_1} \mathcal{E} \quad (20)$$

Similarly, we obtain the polarization phasor  $\mathcal{P}_D$  for the Drude model

$$\mathcal{P}_D = -Nq\mathcal{X} = \frac{-f_0 \epsilon_0 \omega_p^2}{\omega^2 + i\omega\gamma_0} \mathcal{E} \quad (21)$$

and the phasor of the time derivative of  $\mathbf{P}_D$  is represented as

$$-i\omega \mathcal{P}_D = i\omega Nq\mathcal{X} = \frac{i\omega f_0 \epsilon_0 \omega_p^2}{\omega^2 + i\omega\gamma_0} \mathcal{E} \quad (22)$$

The relations in (19) to (22) give the responses of polarizations (and their time derivatives) to electric field in the frequency domain. We then substitute the ansatz of slowly-varying fields [see (8)] for various physical quantities into the instantaneous Poynting theorem [(9) and (16)] and expand around the resonance frequency  $\omega_0$ . To the zeroth order using (19) to (22), we obtain a *positive-definite* effective electric energy and absorption power at the resonance frequency  $\omega_0$  as follows:

$$\begin{aligned} \langle U_e \rangle &\simeq \int_V d\mathbf{r} \frac{\epsilon_0}{2} \left[ \epsilon_{r,\infty} + \frac{f_0 \omega_p^2}{\omega_0^2 + \gamma_0^2} \right. \\ &\quad \left. + \frac{f_1 \omega_p^2 (\omega_0^2 + \omega_1^2)}{(\omega_1^2 - \omega_0^2)^2 + \omega_0^2 \gamma_1^2} \right] \langle \mathbf{E} \cdot \mathbf{E} \rangle \end{aligned} \quad (23a)$$

$$\begin{aligned} \langle P_{\text{abs}} \rangle &\simeq \int_V d\mathbf{r} \epsilon_0 \left[ \frac{f_0 \omega_p^2 \gamma_0}{\omega_0^2 + \gamma_0^2} \right. \\ &\quad \left. + \frac{f_1 \omega_0^2 \omega_p^2 \gamma_1}{(\omega_1^2 - \omega_0^2)^2 + \omega_0^2 \gamma_1^2} \right] \langle \mathbf{E} \cdot \mathbf{E} \rangle \end{aligned} \quad (23b)$$

If more than one Lorentz terms have to be included, we can generalize (23a) and (23b) as

$$\begin{aligned} \langle U_e \rangle &\simeq \int_V d\mathbf{r} \frac{\epsilon_0}{2} \left[ \epsilon_{r,\infty} + \frac{f_0 \omega_p^2}{\omega_0^2 + \gamma_0^2} \right. \\ &\quad \left. + \sum_{i=1}^n \frac{f_i \omega_p^2 (\omega_0^2 + \omega_i^2)}{(\omega_i^2 - \omega_0^2)^2 + \omega_0^2 \gamma_i^2} \right] \langle \mathbf{E} \cdot \mathbf{E} \rangle \end{aligned} \quad (24a)$$

$$\begin{aligned} \langle P_{\text{abs}} \rangle &\simeq \int_V d\mathbf{r} \epsilon_0 \left[ \frac{f_0 \omega_p^2 \gamma_0}{\omega_0^2 + \gamma_0^2} \right. \\ &\quad \left. + \sum_{i=1}^n \frac{f_i \omega_0^2 \omega_p^2 \gamma_i}{(\omega_i^2 - \omega_0^2)^2 + \omega_0^2 \gamma_i^2} \right] \langle \mathbf{E} \cdot \mathbf{E} \rangle \end{aligned} \quad (24b)$$

where  $n$  is the number of Lorentz terms included. The parameters such as  $\omega_i$ ,  $f_i$ ,  $f_0$ ,  $\gamma_i$ ,  $\gamma_0$  and  $\omega_p$  can be found in [24]. In addition, one often works on the narrowband rather than broadband fields. In that case, the dispersion of the material

is fitted with a model containing one Drude term and a finite number of Lorentz terms, as we do in this work.

The same procedures above can be also applied to dispersive and magnetic materials. In this way, the electromagnetic energy for metamaterials are also well defined [15]. Note that the content in the brackets of (24a) is close to the group permittivity in (7b) if the frequency  $\omega_0$  of interest is larger than the damping factor  $\gamma_0$  and far away from the transition frequencies of Lorentz terms.

In the FDTD calculation, when the source is turned off, the total energy  $\langle U_{\text{total}} \rangle$  of a cavity mode will decay exponentially as a function of time. With a long enough period after the source is turned off, we can approximate  $\langle U_{\text{total}} \rangle$  as

$$\langle U_{\text{total}} \rangle = \langle U_e \rangle + \langle U_m \rangle = U_0 \exp\left(-\frac{\omega_0 t}{Q}\right) \quad (25)$$

where  $U_0$  is a constant. In this way, we can obtain the quality factor by extracting the decay parameter. Furthermore, the radiation power and the absorption power are calculated from (7d) and (24b), respectively, and the characteristics of the complicated structure can be analyzed once we obtain the instantaneous fields  $\mathbf{E}$  and  $\mathbf{H}$  from the FDTD method, taking into account the permittivity response function of the material. For the nondispersive dielectric, the content in the brackets of (24a) is replaced with the real part of a constant relative permittivity  $\epsilon_{r,R}$ , and the integral is identical to the conventional definition of the electric energy for nondispersive materials.

In the next section, we will calculate the quality factor of the bowtie antenna using (7a), (7c), (7d), (24a), and (24b) and compare our theoretical results with experimental data.

### III. THE QUALITY FACTOR OF A NANOBOWTIE ANTENNA

The structure of bowtie antenna is shown in Fig. 1 and 2. The bowtie antenna consists of a bottom chromium and a top gold. Their thickness are 3 nm and 21 nm, respectively. The silica is used as the substrate and there is an indium titanium oxide (ITO) layer with 50nm thickness between the bowtie antenna and the silica. In the modeling, the bowtie shape is equitriangular and the curvature radius for each tip is 10 nm. The resonance wavelength from the experimental data is 710 nm, which has been confirmed with our theoretical calculations. We send a plane wave with the resonant wavelength from the substrate into the air. In order to obtain the maximum field enhancement from the plasmonic effect, the polarization of the incident wave is aligned with the tip-to-tip ( $x$ ) direction in Fig. 1. The incident wave runs for 22 optical periods, including 3 periods for the slow turn-on and turn-off, respectively. The turn-on time is set to avoid the excitation of higher-order modes. The remaining running time is long enough for the field to reach the sinusoidal steady state. After the steady state is reached, the source is turned off, but the program keeps running for another 8 optical periods. This duration is long enough to let the residual incident wave propagate in the computation domain and absorbed by the perfect matched layers (PMLs). One optical period has 473 time steps ( $\Delta t=3.33\text{as}$ ) due to a small grid size of 1.5 nm. We record values of electric and magnetic fields each 20 time

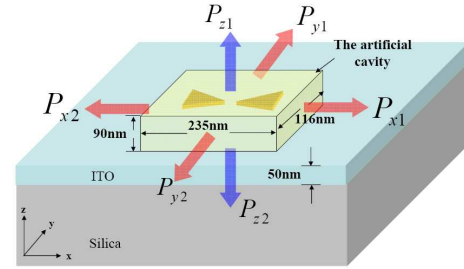


Fig. 1: The artificial cavity and Poynting's vectors for the nanobowtie antenna. The computation domain is surrounded by PMLs.

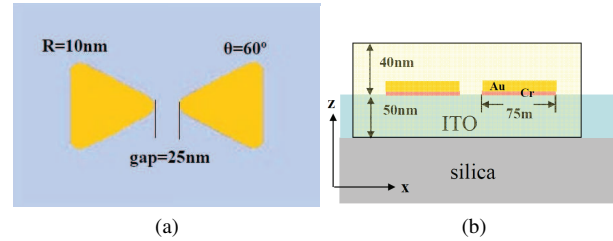


Fig. 2: (a) The top view and (b) side view of the nanobowtie antenna structure. The bowtie antenna is on the indium titanium oxide (ITO) layer with 50nm thickness. The substrate is silica. The bowtie has an equitriangular shape ( $60^\circ$ ) with a radius of curvature 10nm at each corner. The gold thickness is 21nm with a bottom 3nm chromium coating.

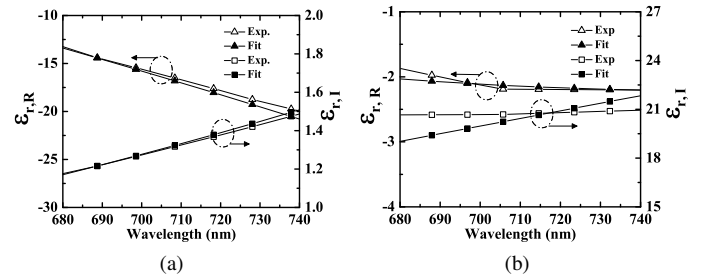


Fig. 3: (a) The permittivity of gold (b) The permittivity of chromium. The experimental data for gold is taken from [25] and the experimental data for chromium is taken from [26].

steps after the source runs for 10 optical periods. Recording values every 20 time steps is accurate enough to describe the field variation in one optical period. In the simulation, the wavelength-dependent refractive indices for the gold and chromium are taken from Ref. [25] and [26], respectively, and we fit the data of gold with the Drude model and data of chromium with the Drude-Lorentz model with a single Lorentz term. The fitting results are shown in Fig.3 and the parameters used are listed in Table I.

Fig. 4 shows the variations of the excited electric field in the gap and the electric field on the incident plane as a function of time. We observe the  $x$  component of electric field at the center of the gap and the middle of metal layer. After the 18th optical period, the source is turned off slowly. The effect of field enhancement can be observed in Fig. 4. In the

TABLE I: Parameters used for fitting the permittivities of gold and chromium. The units for  $\omega_p$  and  $\omega_1$  are  $10^{16}$ rad/s; the units for  $\gamma_0$  and  $\gamma_1$  are  $10^{13}$ rad/s.  $\omega_0=2.65 \times 10^{15}$ rad/s is the resonant angular frequency at  $\lambda=710$  nm. Equations (23a) and (23b) are used.

Metal	$\epsilon_{r,\infty}$	$f_0$	$\omega_p$	$\gamma_0$	$f_1$	$\omega_1$	$\gamma_1$
Au	26.83	1	1.75	8.07	-	-	-
Cr	9.65	0.1	1.63	7.14	0.95	0.17	406.79

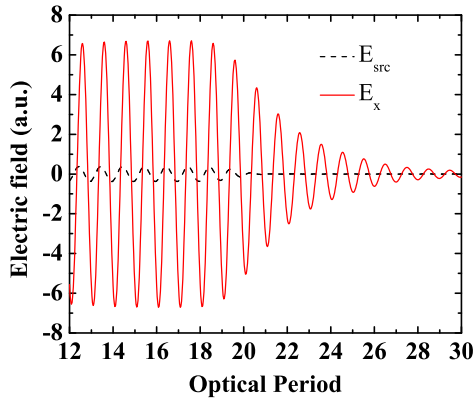


Fig. 4: The  $x$  component of the excited electric field ( $E_x$ ) for bowtie antenna and the electric field ( $E_{src}$ ) from the source as a function of time. The source starts to turned off slowly at the 18th period. The field enhancement factor is around 393.

sinusoidal steady state, the amplitude of the source is around 0.33, and that of the field in the gap is around 6.55. The field enhancement is around 393. After the source is turned off, the field induced by the source starts to decay. Since the source is turned off slowly, we have to wait for several periods so that the residual source wave propagates through the whole computation domain. To see when the residual source wave is completely absorbed by PMLs so that only the resonant mode corresponding to the nanobowtie antenna remains, we calculate the radiation power  $P_{z2}$  as a function of time (Fig. 5). The negative power means that energy is entering the substrate when the source is not completely turned off. After the 20th optical period, the power is positive, and then there is a small competition between the field from the nanobowtie antenna itself and residual source field. After the 21th optical period, the power reaches its maximum, and afterwards, the behavior of the signal comes intrinsically from the nanobowtie antenna. Therefore, we can calculate the stored energy after this moment and observe how long it takes for the stored energy to decay away. This decay time is the lifetime of the energy within this cavity. The longer decay time means a higher quality factor. We can substitute the electric and magnetic fields from the FDTD calculations to obtain the electric energy, (for example, (7b) can be used for calculating electric energy in non-dispersive materials such as ITO and silica; (24a) can be used for calculating electric energy in dispersive materials such as gold and chromium), the magnetic energy (7b), radiation power (7d), and absorption power (24b). The time-dependent stored energy ( $U_{total}$ ) after the source is turned off is shown in Fig. 6. By fitting this curve to (25), we

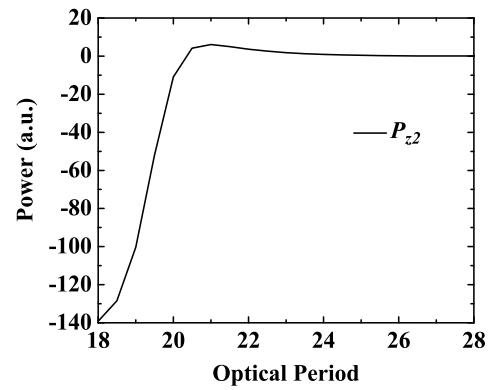


Fig. 5: The radiation power of the bowtie antenna into the substrate as a function of time. The negative power means that the energy is flowing into the bowtie region.

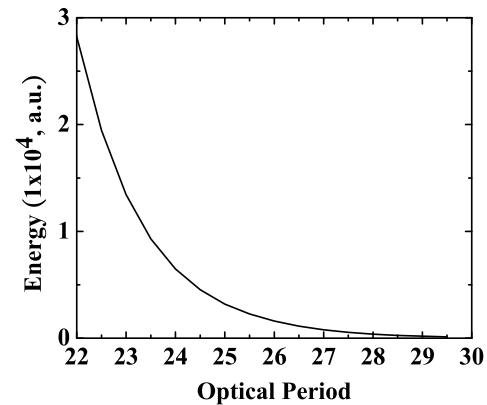


Fig. 6: The stored energy as a function of time. The corresponding quality factor is about 8.74.

obtain a quality factor of 8.74. Comparing this number with the quality factor from the experimental data in Fig. 7, our result is in a reasonable range from 8 to 9. The experimentally-measured quality factors in Fig. 7 are determined directly from darkfield scattering data collected from individual nanobowtie antennas. For the darkfield measurements, white light polarized along the axis of the bowtie was passed through a dark-field oil immersion condenser (Numerical Aperture range=1.2-1.43) onto the nanobowties, which were fabricated on an ITO-coated fused silica substrate. The scattered light was collected in a transmission geometry using a 0.95 NA, 100X air microscope objective. The collected light was then dispersed with a 150 lines/mm grating monochromator onto a liquid-nitrogen-cooled charged coupled device Si detector. Once the resonant wavelength and full width at half maximum (FWHM) are known for a nanobowtie, the quality factor can be evaluated. A detailed description of the nanobowtie fabrication process can be found in reference [2]. The fluctuations in the experimental data are due primarily to variations in nanobowtie structural parameters resulting from fabrication limitations at these length scales

Since we can calculate the radiation and absorption powers of the bowtie nanoantenna, its characteristics can be further investigated. Fig. 8 shows the radiation and absorption powers

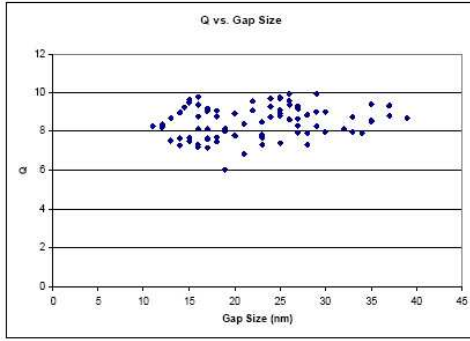


Fig. 7: The dependence of the quality factor of a nanobowtie antenna on the gap size. The experimental data shows that the quality factor is around 8–10.

after the residual field is small enough, that is, the powers come from the cavity mode of bowtie antenna itself. The result indicates that the absorption power is comparable with the radiation power. The reason is that permittivities of gold and chromium at resonant wavelength are  $-17 - 1.3j$  and  $-2.1 - 20.4j$ , respectively, and the large imaginary part of chromium permittivity leads to a significant absorption loss. Although a small field is inside the 3 nm chromium layer, the absorption power is still large. The comparison of the absorption losses due to gold and chromium is shown in Fig. 9(a). From Fig. 9(a), chromium significantly contributes to the absorption loss of the bowtie antenna. As for the radiation loss, the radiation components in different directions are shown in Fig. 9(b). Since the structure is symmetric in both  $x$  and  $y$  directions, we show only the powers  $P_{x1}$  and  $P_{y1}$  radiating into positive  $x$  and  $y$  directions.  $P_{x1}$  is the smallest since the field is confined in this direction due to the metallic bowtie structure. In contrast, there is no feedback in the  $y$  and  $z$  directions. Therefore, the powers  $P_{y1}$ ,  $P_{z1}$  and  $P_{z2}$  are by far larger than  $P_{x1}$ . We also show the radiation patterns of the nanobowtie antenna on the  $x$ - $y$  and  $x$ - $z$  planes in Fig. 10. The patterns are consistent with the results analyzed in the previous section. For example, Fig. 10(b) shows that the radiation power into the substrate is larger than that into the air.

We then calculate the effective modal volume  $V_{\text{eff}}$  with a modified definition for the dispersive materials. The conventional definition for the effective modal volume [27] is

$$V_{\text{eff}} = \frac{\int_V d^3\mathbf{r} \epsilon_{r,R}(\mathbf{r}) |\mathbf{E}(\mathbf{r})|^2}{\max[\epsilon_{r,R}(\mathbf{r}) |\mathbf{E}(\mathbf{r})|^2]} \quad (26)$$

Notice that the numerator and denominator in (26) are total energy and the maximum of the energy density, respectively. Therefore, if dispersive materials are present, the numerator should be replaced with the sum of (24a) [or (7b) if a positive energy is obtainable] and (7c). So is the denominator.

Now the new definition for the effective modal volume is:

$$V_{\text{eff}} = \frac{\int_V d^3\mathbf{r} \frac{1}{2} \epsilon_0 (\epsilon_E(\mathbf{r}, \omega) + \epsilon_{r,R}(\mathbf{r}, \omega)) |\mathbf{E}(\mathbf{r})|^2}{\max[\frac{1}{2} \epsilon_0 (\epsilon_E(\mathbf{r}, \omega) + \epsilon_{r,R}(\mathbf{r}, \omega)) |\mathbf{E}(\mathbf{r})|^2]} \quad (27)$$

, in which the relation below is used:

$$\int_V d\mathbf{r} \frac{\mu_0}{2} |\mathbf{H}(\mathbf{r})|^2 \simeq \int_V d\mathbf{r} \frac{\epsilon_0 \epsilon_{r,R}(\mathbf{r}, \omega)}{2} |\mathbf{E}(\mathbf{r})|^2 \quad (28)$$

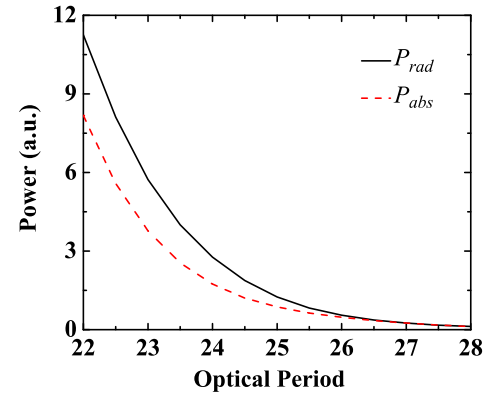


Fig. 8: The radiation and absorption powers of the nanobowtie antenna as a function of time.

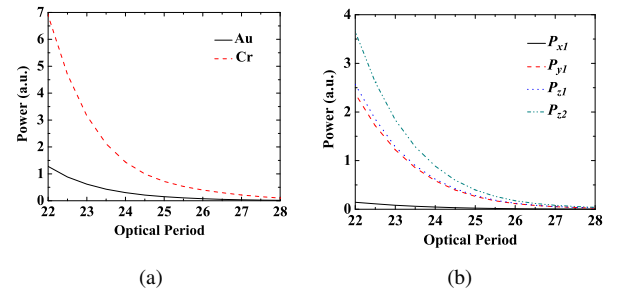


Fig. 9: (a) The absorption powers of gold and chromium as a function of time. (b) The radiation powers into different directions as a function of time.

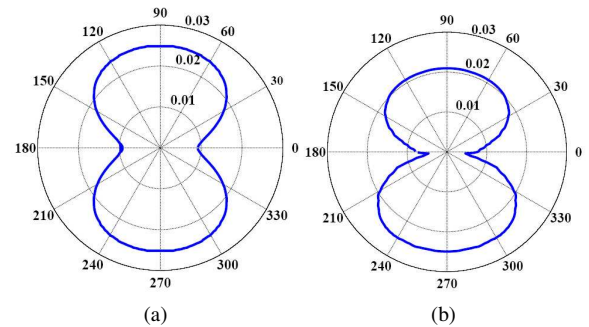


Fig. 10: The radiation pattern of the nanobowtie antenna in the (a)  $x$ - $y$  and (b)  $x$ - $z$  planes, respectively, on the circle with a radius of 150 nm. The angle is measured from the axis along the tip-to-tip ( $x$ ) direction.

and the  $\epsilon_E$  is the coefficient in front of the time-averaged electric intensity in (7b) or (24a).

With this definition, the effective modal volume is  $2.28 \times 10^4 \text{ nm}^3$ , which is equivalent to  $6.36 \times 10^{-5} (\lambda/n_{\text{eff}})^3$ , where  $n_{\text{eff}}$  is the refractive index of the air. This number is far below the diffraction limit. Therefore, even though the quality factor of the nanobowtie antenna is only 8, the ratio of  $Q/V_{\text{eff}}$  is still comparable with those of conventional lasers, which shows that the nanobowtie antenna has the potential to be a nanolaser ([9]).

We summarize the recommended procedures for the calculations of mode properties in an open cavity, such as the

nanoantenna structure based on the FDTD method, as follows:

- 1) Define an artificial cavity which encloses the whole cavity/antenna structure, possibly some portions of the substrate and the covering material.
- 2) Depending on the frequency of interest, using (7b) or (24a), calculate the integrations of the squared magnitude of the instantaneous electric field vector product  $\mathbf{E}(\mathbf{r}, t) \cdot \mathbf{E}(\mathbf{r}, t)$  in the regions with different materials inside the artificial cavity at each time step. Each integration has to be multiplied by the relative group permittivity, which is essential for dispersive media. The sum of each term is the instantaneous electric energy at each time step.
- 3) The result in the previous step contains the slowly- and fast-varying parts. To eliminate the fast-varying part, the time average over half an optical period is performed to obtain the time-averaged electric energy  $\langle U_e \rangle$  corresponding to the slowly-varying part.
- 4) Apply the same procedures to (7c) and (7e) [or (24b)] for  $\langle U_m \rangle$  and  $\langle P_{\text{abs}} \rangle$ , respectively.
- 5) Obtain  $\langle U_{\text{total}} \rangle = \langle U_e \rangle + \langle U_m \rangle$  as a function of time (for example, see Fig. 6). Extract the quality factor by fitting the time dependence of  $\langle U_{\text{total}} \rangle$  to (25).

#### IV. CONCLUSION

In this paper, we use a set of definitions, which are dedicated to the Lorentz-Drude model, for electric energy and absorption power in metals, to calculate the quality factor of a nanobowtie antenna. These definitions always result in positive electric energies in metals over whole wavelength range. The calculated quality factor according to our theory is around 8.74 and is within the range of experimental result. The radiation power, absorption power, and radiation patterns of the nanobowtie antenna are also obtained. Due to the high loss from chromium, the absorption loss is comparable with the radiation loss. In addition, the ultrasmall effective modal volume  $V_{\text{eff}}$  of the nanobowtie antenna has been obtained. The ratio of  $Q/V_{\text{eff}}$  may make nanobowtie lasers possible.

#### ACKNOWLEDGMENT

We thank for many technical discussions with Professors Peidong Yang, Connie Chang-Hasnain, and Ming Wu at the University of California at Berkeley, Professor Cun-Zheng Ning at Arizona State University, Tzy-Rong Lin and Chien-Yao Lu at the University of Illinois at Urbana-Champaign.

#### REFERENCES

- [1] A. Sundaramurthy, K. B. Crozier, G. S. Kino, D. P. Fromm, P. J. Schuck, and W. E. Moerner, "Field enhancement and gap-dependent resonance in a system of two opposing tip-to-tip au nanotriangles," *Phys. Rev. B*, vol. 72, no. 16, p. 165409, May 2005.
- [2] D. P. Fromm, A. Sundaramurthy, P. J. Schuck, G. Kino, and W. E. Moerner, "Gap-dependent optical coupling of single bowtie nanoantenna resonant in the visible," *Nano Lett.*, vol. 4, no. 5, pp. 957–961, March 2004.
- [3] T.-R. Lin, S.-W. Chang, S. L. Chuang, Z. Zhang, and P. J. Schuck, "Coating effect on optical resonance of plasmonic nanobowtie antenna," *Appl. Phys. Lett.*, vol. 97, no. 6, p. 063106, August 2010.
- [4] Z. Rao, L. Hesselink, and J. S. Harris, "High-intensity bowtie-shaped nano-aperture vertical-cavity surface-emitting laser for near-field optics," *Opt. Lett.*, vol. 32, no. 14, pp. 1995–1997, July 2007.
- [5] A. Kinkhabwala, Z. Yu, S. Fan, Y. Avlasevich, K. Müllen, and W. E. Moerner, "Large single-molecule fluorescence enhancements produced by a bowtie nanoantenna," *Nano Lett.*, vol. 3, pp. 654–657, October 2009.
- [6] J. Merlein, M. Kahl, A. Zuschlag, A. Sell, A. Halm, J. Boneberg, P. Leiderer, A. Leitenstorfer, and R. Bratschitsch, "Nanomechanical control of an optical antenna," *Nature Photonics*, vol. 2, pp. 230–233, April 2008.
- [7] Z. Zhang, A. Weber-Bargioni, S. W. Wu, S. Dhuey, S. Cabrini, and P. J. Schuck, "Manipulating nanoscale light fields with the asymmetric bowtie nano-colorsorter," *Nano Lett.*, vol. 9, pp. 4505–4509, November 2009.
- [8] N. Yu, E. Cubukcu, L. Diehl, D. Bour, S. Corzine, J. Z. G. Hoffer, K. Crozier, and F. Capasso, "Bowtie plasmonic quantum cascade laser," *Opt. Express*, vol. 15, no. 20, pp. 13 272–13 281, October 2007.
- [9] S. W. Chang, C. Y. A. Ni, and S. L. Chuang, "Theory for bowtie plasmonic nanolasers," *Optics Express*, vol. 16, no. 14, pp. 10 580–10 595, July 2008.
- [10] S. W. Chang and S. L. Chuang, "Normal modes for plasmonic nanolasers with dispersive and inhomogeneous media," *Opt. Letters*, vol. 34, pp. 91–93, January 2009.
- [11] L. D. Landau and E. M. Lifshitz, *Electrodynamics of Continuous Media*. Pergamon Press, Oxford, 1960.
- [12] J. D. Jackson, *Classical Electrodynamics*. New York: Wiley, 1999.
- [13] R. Loudon, "The propagation of electromagnetic energy through an absorbing dielectric," *J. Phys. A: Gen. Phys.*, vol. 3, no. 3, pp. 233–245, May 1970.
- [14] R. Ruppin, "Electromagnetic energy density in a dispersive and absorptive material," *Phys. Lett. A*, vol. 299, no. 2-3, pp. 309–312, July 2002.
- [15] T. J. Cui and J. A. Kong, "Time-domain electromagnetic energy in a frequency-dispersive left-handed medium," *Phys. Rev. B*, vol. 70, no. 20, p. 205106, November 2004.
- [16] A. D. Boardman and K. Marinov, "Electromagnetic energy in a dispersive metamaterial," *Phys. Rev. B*, vol. 73, no. 16, p. 165110, April 2006.
- [17] A. Taflov and S. C. Hagness, *Computational Electrodynamics: The Finite-Difference Time-Domain Method*. Artech House, 2000.
- [18] A. Farjadpour, D. Roundy, A. Rodriguez, M. Ibanescu, P. Bermel, J. D. Joannopoulos, S. G. Johnson, and G. Burr, "Improving accuracy by subpixel smoothing in FDTD," *Opt. Lett.*, vol. 31, no. 20, pp. 2972–2974, October 2006.
- [19] C. A. Balanis, *Advanced Engineering Electromagnetics*, 1st ed. Wiley, New York, 1989.
- [20] P. H. Harms, Y. Shimony, and R. Mittra, "Computing the quality factor of resonators using the finite-difference-time-domain algorithm," *Microw. Opt. Tech. Lett.*, vol. 11, no. 2, pp. 64–66, December 1998.
- [21] S. Collardey, A. Sharaiha, and K. Mahdjoubi, "Evaluation of antenna radiation Q using FDTD method," *Elec. Lett.*, vol. 41, no. 12, pp. 675–677, June 2005.
- [22] C. A. Grimes, F. T. G. Liu, and D. M. Grimes, "Time-domain measurement of antenna Q," *Microw. Opt. Tech. Lett.*, vol. 25, no. 2, pp. 95–100, March 2000.
- [23] V. Mandelstam and H. S. Taylor, "Harmonic inversion of time signals and its applications," *J. Chem. Phys.*, vol. 107, no. 17, pp. 6756–6769, November 1997.
- [24] A. D. Rakić, A. B. Djurišić, J. M. Elazar, and M. L. Majewski, "Optical properties of metallic films for vertical-cavity optoelectronic devices," *Appl. Opt.*, vol. 37, no. 22, pp. 5271–5283, August 1998.
- [25] E. D. Palik, *Handbook of Optical Constants of Solids*. New York: Academic, 1985.
- [26] P. B. Johnson and R. W. Christy, "Optical constants of transition metals: Ti, v, cr, mn, fe, co, ni, and pd," *Phys. Rev. B*, vol. 9, no. 12, pp. 5056–5070, June 1974.
- [27] J. S. Foresi, P. R. Villeneuve, J. Ferrera, E. R. Thoen, G. Steinmeyer, S. Fan, J. D. Joannopoulos, L. C. Kimerling, H. I. Smith, and E. P. Ippen, "Photonic-bandgap microcavities in optical waveguides," *Nature*, vol. 390, pp. 143–145, September 1997.

**Chi-Yu Adrian Ni** received the B.S. degree in the Department of Electrical Engineering in 2000, and M.S. degree at the Graduate Institute of Photonics and Optoelectronics in 2002, respectively, both from National Taiwan University. After graduated from National Taiwan University, he joined the Opto-Electronic Epitaxy and Device Department at Industrial Technology Research Institute (ITRI), Hsinchun, Taiwan, as an associate engineer from 2002 to 2006. He began his PhD study in the Department of Electrical and Computer Engineering, the University of Illinois at Urbana-Champaign in 2007 and is currently a PhD candidate. His research interest is in the area of semiconductor physics, mainly in optoelectronics including plasmonic devices, lasers, and modulators.



**Shun Lien Chuang** (S'78–M'82–SM'88–F'97) received the B.S. degree from National Taiwan University, Taipei, in 1976, and the M.S., E.E., and Ph.D. degrees from the Massachusetts Institute of Technology, Cambridge, in 1980, 1981, and 1983, respectively, all in electrical engineering.

In 1983, he joined the Department of Electrical and Computer Engineering at the University of Illinois at Urbana-Champaign, Urbana, where he is currently the Robert MacClinchie Distinguished Professor. He was a visitor at AT&T Bell Laboratories (1989), the SONY Research Center (1995), and NTT Basic Research Laboratories (1997). He was also a visitor at NASA Ames Research (1999), Fujitsu Research Laboratories (2000), Cavendish Laboratory at the University of Cambridge (2002), and the Technical University of Berlin (2009). He contributed to the theory of strained quantum well, band structures and optical gain models. He is conducting research on nanolasers, plasmonics, strained semiconductor quantum-well and quantum-dot lasers, and superlattice photodetectors. He is the author of *Physics of Photonic Devices* (Wiley, 2009, second edition) and *Physics of Optoelectronic Devices* (Wiley, 1995, first edition). He has published more than 300 journal and conference papers and given many invited talks at conferences and institutions.

Dr. Chuang is a Fellow of the American Physical Society and the Optical Society of America. He has been cited many times for Excellence in Teaching at the University of Illinois. He was also awarded a Fellowship from the Japan Society for the Promotion of Science to visit the University of Tokyo in 1996. He received the Engineering Excellence Award from the Optical Society of America in 2004, the IEEE Lasers and Electro-Optical Society (LEOS) Distinguished Lecturer Award for 2004-2006 for two terms, and the William Streifer Scientific Achievement Award from IEEE (LEOS) in 2007. He received the Humboldt Research Award for Senior U.S. Scientists in 2008-2009. He was elected as a member of the Board of Governors for IEEE Photonics Society for 2009-2011. He served as an Associate Editor of the IEEE JOURNAL OF QUANTUM ELECTRONICS (1997-2002) and the JOURNAL OF LIGHTWAVE TECHNOLOGY (2007-2008). He was a General Co-Chair for Slow and Fast Light Meeting of the Optical Society of America, July, 2008 and has served in many technical program committees of IEEE and Optical Society of America. He was a Feature Editor for a special issue in *Journal of Optical Society of America B on Terahertz Generation, Physics and Applications* in 1994. He also edited a feature section on Mid Infrared Quantum-Cascade Lasers in the June 2002 issue of the *Journal of Quantum Electronics*.

**Shu-Wei Chang** (M'09) received the B.S. degree in electrical engineering from National Taiwan University, Taipei, in 1999, and the M.S. and Ph.D. degrees from the Department of Electrical and Computer Engineering, University of Illinois at Urbana-Champaign, Urbana, in 2003 and 2006, respectively. He received the John Bardeen Memorial Graduate Award from the same department in 2006. Dr. Chang is a member of IEEE and Optical Society of America. His research interest is mainly in the fundamental and applied physics of semiconductor photonics including tunneling-injection quantum-dot-quantum-well coupled system, slow and fast light in semiconductor nanostructures, spin relaxation in strained [110] and [111] semiconductor quantum wells, and group IV direct-bandgap semiconductor lasers, active and passive plasmonic devices, and semiconductor nanolasers.

**P. James Schuck** earned his B.A. in Physics at UC Berkeley in 1997, and his M.S. and Ph.D. in Applied Physics at Yale University in 1998 and 2003, respectively, where he worked in the group of Prof. Robert Grober. After obtaining his Ph.D., he spent three years as a postdoctoral researcher at Stanford University, where he was advised by Prof. W. E. Moerner studying optical nanoantennas and single-molecule spectroscopy. He is currently a Staff Scientist at the Molecular Foundry located at Lawrence Berkeley National Laboratories, where he has established the Nano-optics Lab within the Imaging and Manipulation of Nanostructures Facility. His research currently focuses on nano-photonic/plasmonic device applications and nanoscale optical imaging spectroscopy of novel materials, investigating the interactions of light and nanoscale objects.